Generalized Two-Sided Linear Prediction Approach for Land Mine Detection

Thomas C. T. Chan*, H. C. So* and K. C. Ho†
*Department of Electronic Engineering, City University of Hong Kong
Tat Chee Avenue, Kowloon, Hong Kong
†Department of Electrical and Computer Engineering University of Missouri-Columbia
Columbia, MO 65211, USA

August 7, 2007

Keywords : land mine detection, linear prediction, ground penetrating radar

Abstract : Ground penetrating radar (GPR) is a widely used sensor for land mine detection. However, GPR signal return is very susceptible to ground bounce and reflection of clutter objects, which makes the detection a difficult problem to date. In this paper, we propose to utilize two-sided linear prediction (LP) to model the background interference and then employ the residue energy to generate the test statistic. It is demonstrated from real GPR data that the proposed scheme is able to significantly suppress the interference due to ground reflection and is superior to the adaptive ground bounce removal and one-sided LP methods.

1 Introduction

Since World War II, numerous conflicts in Europe, Africa, Central and South America, the Middle East and Asia resulted in the planting of millions of land mines. It is important to locate these mines that can potentially cause massive number of deaths and casualties.

Owing to the capabilities of good penetration and depth resolution as well as detecting both metallic and nonmetallic objects, ground penetrating radar (GPR) [1] has been considered as a viable technology for land mine detection. A GPR system consists of a transmitter for emitting electromagnetic wave to the inspection surface and a receiver for collecting the returned signal from which the decision of whether there is a mine is made. However, detecting land mines with GPR is still a difficult task because on one hand strong reflections from the ground surface dominate the mine response particularly when the mines are deeply buried. On the other hand, it could be intractable to differentiate a land mine and a clutter object even if the ground bounce is successfully removed. As a result, signal processing is a crucial step for rendering the GPR sensor outputs to increase probability of detection and/or reduce false alarm rate. Over the years, many signal processing algorithms have been proposed for GPR data. Some of them are the hidden Markov model (HMM) [2] that is designed to detect the hyperbolic signature produced from a land mine, the least mean square (LMS) algorithm [3] that detects anomaly in the soil background, and the principal component analysis (PCA) [4] that is used to model the soil background. Enhancing land mine signal through digital filtering is proposed in [5]. Feature based algorithms together with training are also developed recently [6]-[8]. More related to our work on eliminating the soil background for land mine detection, Wu *et al* [9] have proposed to remove the ground bounce response by modeling it as a shifted and scaled version of an adaptively estimated reference ground bounce. Alternatively, a constant false alarm rate detector based on modeling the background and clutter reflection by one-sided linear prediction (LP) has been derived in [10]. It is noteworthy that apart from the commonly used one-sided LP, two sided LP [11] can also be used for parameter estimation. In this paper, we extend the LP idea to devise a novel land mine detection algorithm. Unlike [10] which processes GPR signals using the standard one-sided LP in frequency domain, we propose a generalized version of two-sided LP and employ it to perform processing in spatial domain. It is shown that the proposed detector is superior to [9] and [10] and has high potential of reducing false alarm probability.

2 Two-Sided Linear Prediction Approach

This section describes the proposed two-sided LP method. In our study, we consider the GPR data sets at [12] which were obtained by measuring the time domain response from an impulse GPR with a center frequency of around 1GHz. Each experimental setup of [12] contains land mines and other clutter objects including large stone, empty cartridge, and/or copper wire strip. The top view of a typical setup is depicted in Figure 1. The data set contains the GPR response from 51 channels with uniform spacing of 1 cm in the y-axis and we see that all of them were centered on the 25th channel. Each channel or B-scan is composed of a linear sequence of 196 A-scans. Each A-scan is the GPR response with respect to time (i.e., depth) at a given x-position, and adjacent A-scans were separated by 1 cm. The B-scan of the 25th channel is shown in Figure 2 where the horizontal axis and vertical axis correspond to the scan and depth, respectively, with approximately 512 depth pixels. Apparently, it is difficult to perform mine detection by observing Figure 2.

Let the GPR response return vector in the direction of depth be $\mathbf{d}(x, y)$ where x and y represent the dimensions of scan and channel, respectively. The task of land mine detection can be casted as the following binary hypothesis test:

$$\begin{array}{l} H_0 : \mathbf{d}(x, y) = \mathbf{g}(x, y) + \mathbf{q}(x, y) \\ H_1 : \mathbf{d}(x, y) = \mathbf{s}(x, y) + \mathbf{g}(x, y) + \mathbf{q}(x, y) \end{array} \tag{1}$$

where $\mathbf{g}(x, y)$ represents the composite of the background and/or clutter response and the antenna internal coupling components, $\mathbf{q}(x, y)$ denotes measurement noise at the GPR antenna and $\mathbf{s}(x, y)$ is the response from a mine. That is, we assume that $\mathbf{d}(x, y)$ is a linear combination of $\mathbf{g}(x, y)$ and $\mathbf{q}(x, y)$, and also $\mathbf{s}(x, y)$ if a mine is present. In practical situation, the GPR data are collected at very high signal-to-noise ratio and thus the effect of $\mathbf{q}(x, y)$ is negligible, while the background is the dominant response in both hypotheses. We shall simply call $\mathbf{g}(x, y)$ the interference in sequel.

The basic assumption of our methodology is that the interference, $\mathbf{g}(x, y)$, can be modeled using two-sided LP while $\mathbf{s}(x, y)$ cannot, and experimental results demonstrate the effectiveness of our proposal. We will first subtract an estimate of $\mathbf{g}(x, y)$ formed using the two-sided LP model. Then the energy of the residue signal will be utilized to decide if each location,(x, y), falls under H_1 or H_0.

We propose to employ the following two-coefficient LP model in the scan direction to approximate $\mathbf{g}(x, y)$:

$$\mathbf{g}(x, y) \approx a_{p_-}(x)\mathbf{g}(x-p, y) + a_{p_+}(x)\mathbf{g}(x+p, y) \tag{2}$$

where the LP step-size, $p \geq 1$ is chosen based on the size of suspected mines. The two-sided LP model has two advantages over the one-sided LP model. First, more accurate estimation of $\mathbf{g}(x, y)$ is expected because samples from both the past, $\mathbf{g}(x-p, y)$, and the future, $\mathbf{g}(x+p, y)$, are used. This is analogous to [11] which proves that two-sided LP produces smaller residuals than one-sided LP for any wide-sense stationary random process. It is worthy to mention that we allow $a_{p_-}(x) \neq a_{p_+}(x)$ which generalizes the common practice of symmetric coefficients in two-sided LP model from [11], and thus an even better modeling is anticipated. Second, it is able to suppress the response of clutter objects that are larger in size than typical land mines. That is, by setting p according to the size of typical land mines, the response of large clutter objects can fit to the model of (2) as well. However, it is critical that the value of p should be chosen larger than half of the horizontal length of the detection target divided by the spatial resolution. If p is set too small, the response of the target will fit the model of (2), and will be estimated as a background response. On the other hand, when p is chosen to be too big, the modeling of the $\mathbf{g}(x, y)$ will be less accurate due to the gradual changing variations in the background.

Denoting

$$\mathbf{G}_p(x, y) = [\mathbf{g}(x-p, y)\ \mathbf{g}(x+p, y)]^H \tag{3}$$

and

$$\mathbf{a}_p(x) = \begin{bmatrix} a_{p_-}(x) \\ a_{p_+}(x) \end{bmatrix} \tag{4}$$

where H denotes the complex conjugate transpose operator. From (2)$-$(4), we have:

$$\mathbf{g}(x, y) \approx \mathbf{G}_p^H(x, y)\ \mathbf{a}_p(x) \tag{5}$$

Assuming the hypothesis of H_0, according to (1) $\mathbf{d}(x, y)$ is close to $\mathbf{g}(x, y)$ since the noise component $\mathbf{q}(x, y)$ is sufficiently small. The estimate of $\mathbf{a}_p(x)$, denoted by $\hat{\mathbf{a}}_p(x)$, is computed using standard least squares as

$$\hat{\mathbf{a}}_p(x) = \left(\mathbf{D}_p(x, y)\mathbf{D}_p^H(x, y)\right)^{-1} \mathbf{D}_p(x, y)\mathbf{d}(x, y) \tag{6}$$

where $\mathbf{D}_p(x, y) = [\mathbf{d}(x - p, y)\ \mathbf{d}(x + p, y)]^H$. The estimated background under H_0 then becomes

$$\hat{\mathbf{g}}(x, y) = \mathbf{D}_p^H(x, y)\hat{\mathbf{a}}_p(x) \tag{7}$$

The residue signal vector which is obtained by subtracting $\hat{\mathbf{g}}(x, y)$ from $\mathbf{d}(x, y)$, denoted by $\mathbf{h}(x, y)$, is:

$$\mathbf{h}(x, y) \quad = \mathbf{d}(x, y) - \hat{\mathbf{g}}(x, y) \tag{8}$$

With the assumption that the interference is accurately estimated, $\mathbf{h}(x, y) \approx \mathbf{q}(x, y)$ under H_0 and $\mathbf{h}(x, y) \approx \mathbf{s}(x, y) + \mathbf{q}(x, y)$ under H_1. Therefore, it is expected that the energy of $\mathbf{h}(x, y)$ will be much larger when a land mine is present. As a result, the residue energy in the vicinity of a suspected scan position x, denoted by $\varepsilon(x)$, is utilized in producing the test statistic:

$$\varepsilon(x) = \frac{1}{N} \sum_{n=y_0-\frac{N-1}{2}}^{y_0+\frac{N-1}{2}} \mathbf{h}^H(x, n)\mathbf{h}(x, n) \tag{9}$$

where N is the number of channels to be averaged and its value should be chosen sufficiently large to cover the mine target. While y_0 is the center of the suspected location that may contain a mine. Thus, by setting the averaging area comparable to land mine size, we can reduce the false detection from clutter objects that are smaller in size. It should be noted that the proposed method requires some prior information about the land mine targets to be detected, in order to set the prediction step-size p and the averaging size N properly to achieve better performance.

3 Results and Discussions

The proposed method was first tested on the setup in Figure 1, which is referred to as Scenario 1. The objects, namely, the PMA-3 mine, large stone, PMA-1 mine, and copper strip were centered on the 25th, 75th, 125th, and 175th scan, respectively, and were buried 5 cm deep in clay mixed with small rocks. Since all of them were centered on the 25th channel, $y_0 = 25$ was chosen. The surface of the clay was smoothed, but there is a difference of approximately 10 cm between the highest and lowest ground levels with irregularities throughout. The GPR antenna was placed 5 cm above the highest ground level during the scan process. The GPR data were collected after 23 days with the clay still moist. Unless stated otherwise, p and N were set to 10 and 9, respectively, according to our prior knowledge that the PMA-3 mine had a 10 cm diameter and the PMA-1 mine had length of 14 cm and width of 7 cm.

The effect of the value of p on the proposed scheme was first examined and Figure 3 plots the residue energy of (9) versus scan location for p equal 20, 10 and 4. It is observed from the top figure that if p was set to too large, the overall residue energy increased even over background region (for example, around the 150th scan). On the other hand, as shown from the bottom figure, the peaks of the residue energy corresponding to the locations of the land mines decreased when p was chosen to too small. While the choice of $p = 10$ was the best among the three values and this agrees with our discussion in Section 2 that it must be greater than half of the length of the land mine in the unit of spatial resolution.

The comparative performance of the proposed scheme and the adaptive ground bounce removal (AGBR) algorithm [9] as well as the one-sided LP method [10] with only one coefficient with $p = 10$ was then examined. The test statistics of all three methods were computed using (9) and the results are shown in Figure 4. It is immediately realized that the residue from the stone (around x=75 cm) was quite small in all three algorithms. In order to understand better the reason behind, Figures 5 and 6 show the B-scans and projected energies along time, respectively, of the estimated object responses after local background removal. (Local background removal simply averages a few scans in close proximity before and after an object and subtracts the average from the data containing the object.) Figure 5 clearly indicates the presence of the response from the stone (second subfigure), it also shows significant variation in the background from $x = 160$ cm to 190 cm in which local background removal failed to remove the background. From Figure 6, however, we see that the responses of the stone and the copper wire were smaller than those of the mines.

From Figure 4, it is observed that the performance of the AGBR and one-sided LP methods was not satisfactory for $x \in (161, 190)$ cm, which implied their ineffective background suppression in this region as the estimated energy of the copper strip was relatively small. While the proposed method not only removed the ground surface response under more stable conditions, that is, from $x = 1$ to $x = 160$ cm, but was also able to track and remove the rapidly changing background response which corresponded to $x \in (161, 190)$ cm. In addition, the one-sided LP method undesirably provided double peaks at the two mines as well as the large stone, which further indicated its inferiority over the two-sided LP approach.

Along with the setup in Figure 1, another set of data obtained from [12] was also tested. In this setup, which is referred to as Scenario 2, an empty cartridge replaced the large stone and the clay condition is that it is completely dry with a few cracks. Figure 7 shows the test statistics of the three methods and we again see that the proposed approach outperformed the the AGBR and one-sided LP schemes.

Table 1 summarizes and combines the results from both setups in comparing the false alarm rates for detecting the four land mine targets. We consider that the target area to be ±8 cm from the center of the 4 land mines while the remaining was assumed target free area. The false alarm rate was calculated by the number of false detections divided by the number of target free scans. Based on these two sets of GPR data, the proposed method gave the best detection performance.

Number of land mines detected	False alarm rate		
	AGBR	One-sided LP	Two-sided LP
4	9.33%	5.00%	0.00%
3	8.00%	2.67%	0.00%
2	7.33 %	2.67%	0.00%
1	4.67%	0.67%	0.00%

Table 1: False alarm rates for three methods

4 Conclusion

A generalized two-sided linear prediction (LP) approach has been proposed to model the background interference in ground penetrating radar returns. After removing the interference, the response from mines can be extracted. Experimental results show that the proposed method can suppress and track the interference and ground reflection, and is superior to the adaptive ground bounce removal and one-sided LP schemes.

Acknowledgement

The authors would like to thank the anonymous reviewers for their helpful and constructive comments that improved the clarity of the paper. The work described in this paper was fully supported by a grant from the Research Grants Council of the Hong Kong Special Administrative Region, China [Project No. CityU 119605].

References

[1] T.R. Witten "Present state of the art in ground-penetrating radars for mine detection," *in Proc. SPIE Conf.*, vol.3392, pp.576-586, Orlando, FL, 1998

[2] P.D. Gader, M. Mystkowski, Yunxin Zhao, "Landmine detection with ground penetrating radar using hidden Markov models," *IEEE Trans. Geosci. Remote Sensing*, vol.39, no.6, pp.1231-1244, June 2001

[3] P. Torrione, L. Collins, F. Clodfelter, S. Frasier and I. Starnes, "Application of the LMS algorithm to anomaly detection using the Wichmann/Niitek ground penetrating radar," *in Proc. SPIE Detection and Remediation Technologies for Mines and Minelike Targets*, vol.VIII, pp. 1127 - 1136, Orlando, Apr. 2003

[4] S. Yu, R.K. Mehra and T.R. Witten, "Automatic mine detection based on ground penetrating radar," *in Proc. of SPIE, Detection and Remediation Technologies for Mines and Minelike Targets*, vol.IV, pp. 961-972, Orlando, FL, Apr. 1999

[5] D. Potin, E. Duflos and P. Vanheeghe, "Landmines ground-penetrating radar signal enhancement by digital filtering," *IEEE Transactions on Geoscience and Remote Sensing*, vol.44, no.9, pp.2393-2406, Sept. 2006

[6] P.D. Gader, W. Lee and J.N. Wilson, "Detecting landmines with ground-penetrating radar using feature-based rules, order statistics, and adaptive whitening," *IEEE Trans. Geosci. Remote Sensing*, vol.42, no.11, pp.2522-2534, Nov. 2004

[7] H. Frigui and P. D. Gader, "Detection and discriminatiokn of land mines based on edge histogram descriptors and fuzzy K-nearest neighbors," *in Proc. IEEE Int. Conf. Fuzzy Systems*, pp.1494-1499, Vancouver, 2006

[8] W.-H. Lee, P.D. Gader and J.N. Wilson, "Optimizing the area under a receiver operating characteristic curve with application to landmine detection," *IEEE Trans. Geosci. Remote Sensing*, vol.45, no.2, pp.389-397, Feb. 2007

[9] R. Wu, A. Clement, J. Li, E.G. Larsson, M. Bradley, J. Habersat and G. Maksymonko, "Adaptive ground bounce removal," *Electronics Letters*, vol.37, no.20, pp.1250-1252, 2001

[10] K.C. Ho and P.D. Gader, "A linear prediction land mine detection algorithm for hand held ground penetrating radar," *IEEE Trans. Geosci. Remote Sensing*, vol.40, no.6, pp.1374-1384, 2002

[11] J.-J Hsue and A.E. Yagle, "Similarities and differences between one-sided and two-sided linear prediction," *IEEE Trans. Signal Processing*, vol.43, no.1, pp.345-349, 1995

[12] http://www.minedet.etro.vub.ac.be/groundbase/datafiles/html/datafiles.html

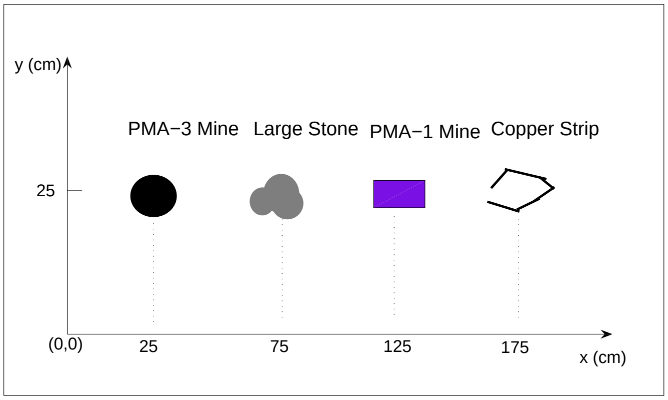

Figure 1: GPR data setup adapted at [12] (Scenario 1)

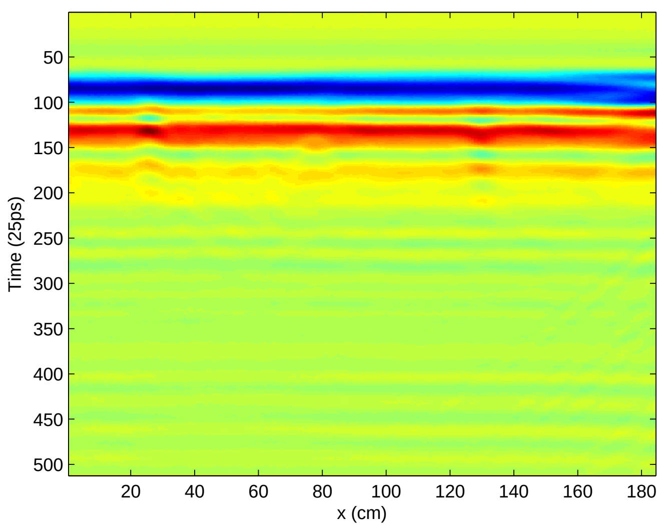

Figure 2: B-scan of GPR data

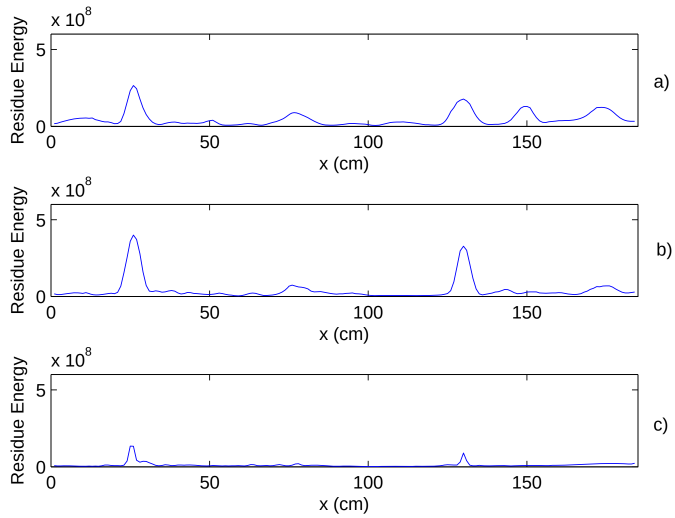

Figure 3: Residue energy versus scan location: (a) $p = 20$, (b) $p = 10$, (c) $p = 4$

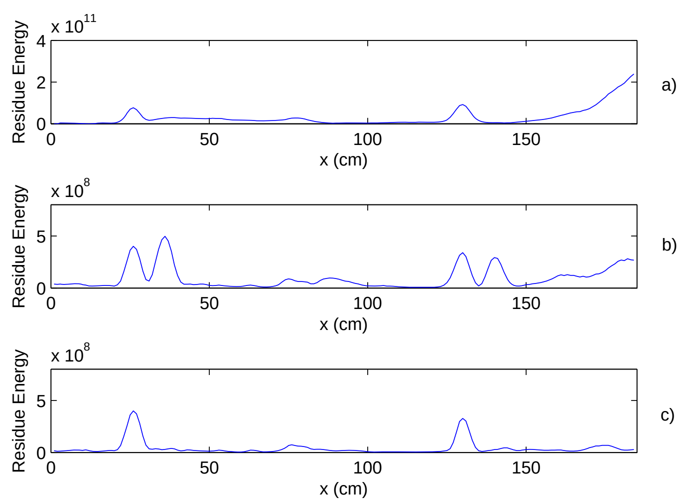

Figure 4: Residue energy versus scan location (Scenario 1): (a) AGBR, (b) one-sided LP, (c) two-sided LP

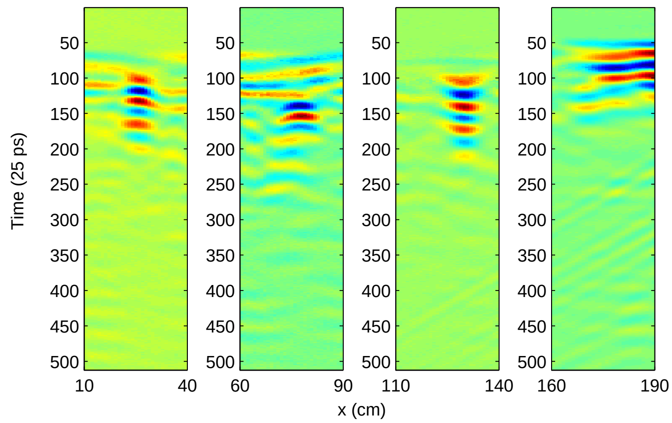

Figure 5: B-scans of targets after local background removal

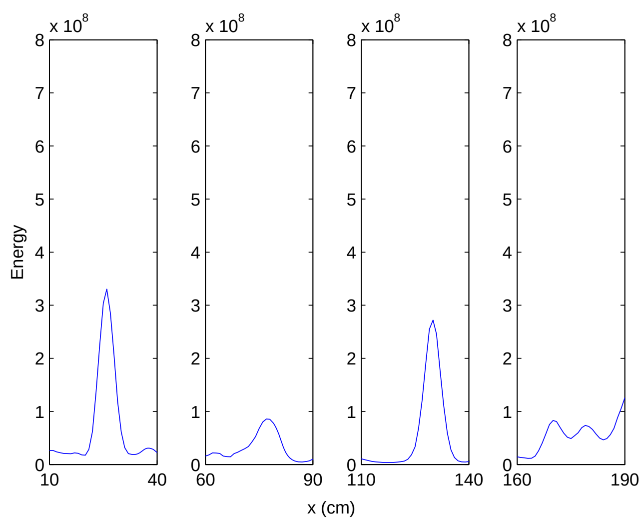

Figure 6: Energies of targets after local background removal

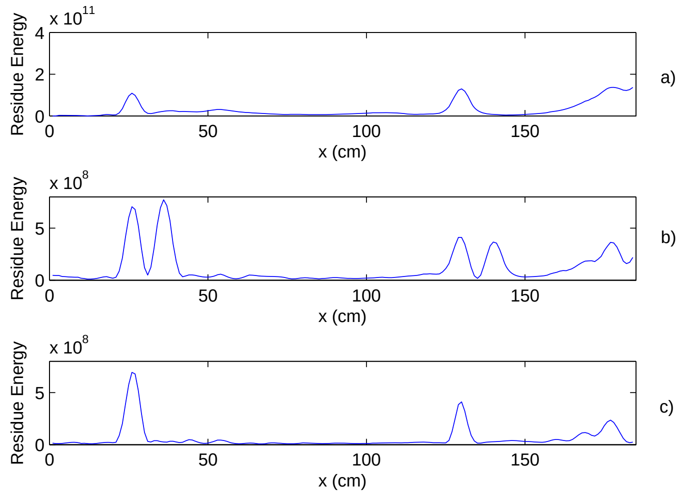

Figure 7: Residue energy versus scan location (Scenario 2): (a) AGBR, (b) one-sided LP, (c) two-sided LP